An Integrate-and-Fire Model for Synchronized Bursting in a Network of Cultured Cortical Neurons

D.A. French

Department of Mathematical Sciences, University of Cincinnati, Cincinnati, OH 45221-0025

E.I. Gruenstein

College of Medicine, University of Cincinnati, Cincinnati, OH 45221-0524

February 6, 2005

Abstract

It has been suggested that spontaneous synchronous neuronal activity is an essential step in the formation of functional networks in the central nervous system. The key features of this type of activity consist of bursts of action potentials with associated spikes of elevated cytoplasmic calcium. These features are also observed in networks of rat cortical neurons that have been formed in culture. Experimental studies of these cultured networks have led to several hypotheses for the mechanisms underlying the observed synchronized oscillations. In this paper, bursting integrate-and-fire type mathematical models for regular spiking (RS) and intrinsic bursting (IB) neurons are introduced and incorporated through a small-world connection scheme into a two-dimensional excitatory network similar to those in the cultured network.

This computer model exhibits spontaneous synchronous activity through mechanisms similar to those hypothesized for the cultured experimental networks. Traces of the membrane potential and cytoplasmic calcium from the model closely match those obtained from experiments. We also consider the impact on network behavior of the IB neurons, the geometry and the small world connection scheme.

Keywords: Integrate-and-fire, cultured cortical network, spontaneous synchronized oscillations.

1. Introduction:

The development of organized structures such as neuronal networks in the central nervous system (CNS) is an important area of research in Neuroscience. It has been suggested that spontaneous synchronized activity is an essential step in the formation of a functional network (Katz and Shatz, 1996). This type of *in vivo* activity, though not well understood (Tabak et al, 2000), is also observed in networks of rat cortical neurons found in culture (for a review, see Feller (1999)). Because of this similarity it is possible that studies of these cultured *in vitro* networks will provide a model system leading to a better understanding of the developing CNS.

Experimentally observed spontaneous network activity is typically characterized by electrical bursting events accompanied by significant "spikes" in the levels of intracellular calcium. Each of these events is separated by a quiescent period, typically lasting for several seconds but which may be as much as a minute in duration. The burst events are synchronized throughout the network even though the individual action potentials (APs) that comprise each burst are not. On a global level each spontaneous event is characterized

by a rapid wavelike spread of APs throughout the network with a different neuron initiating each burst (Maeda et al, 1995).

Synaptic events are thought to provide the primary mechanism for the initiation and control of these bursting events. In particular, background noise in the form of miniature excitatory postsynaptic potentials (mEPSPs) along with a constant depolarizing current due to tonic NMDA receptor activity may be of particular importance (Robinson et al, 1993a; Robinson et al, 1993b or Wang and Gruenstein, 1997).

The behavior that our model seeks to emulate is derived largely from the behavior of the *in vitro* neuronal networks described by Maeda et al (1995), Murphy et al (1992), Opitz et al (2002), Robinson et al (1993a), Robinson et al (1993b), Voigt et al (2001), and Wang and Gruenstein (1997). In those reports dissociated neurons from embryonic rat cortex gradually reassociate to form a synaptically connected network. After several days in culture this developing network displays occasional AP bursts with associated calcium spikes. After 7-10 days *in vitro* these events become regular, global, and synchronized. The rising phase of each calcium spike is associated with a burst of APs. In none of the studies to date has evidence for a pacemaker that would drive the oscillations been reported. This is suggestive of a stochastic, noise based mechanism for generation of these events. If the events are triggered by random noise the initiation sites will tend to vary from burst to burst as well as the intervals between bursts (This is also observed in the retina; see Feller et al, 1997).

In this paper we will use simulations based on a mathematical model with integrate-and-fire neurons to explore the mechanisms for the synchronized activity. Recently, computational neuroscientists have begun to use integrate-and-fire methods to model phenomenon such as bursting and calcium oscillations (Coombs et al, 2001; Laing and Longtin, 2002; Liu and Wang, 2001; or van Vreeswijk and Hansel, 2001). Here we consider excitatory networks consisting of RS and IB cortical neurons as described in McCormick et al (1985).

The primary goal of this work is to create a plausible model for the synchronous oscillatory behavior of these cultured cortical networks. A secondary goal has been to extend integrate-and-fire modeling. We introduce a special refractory mechanism which allows the firing rates of integrate-and-fire neurons more closely to match those observed in the experimental studies. We also used a low threshold current to create IB neurons. These integrate-and-fire type neurons respond to a small, short current pulse with a burst of several APs. We also were interested in the geometry, which, in contrast to many other computational studies is fully two-dimensional. Our connection scheme is local with some random rewiring according to a probability parameter ρ. We consider, in particular, the impact of ρ and the IB neurons.

2. Methods:

In this section we describe our mathematical model for a network of cultured neurons. We assume that the neurons in the cultured network are primarily pyramidal cells and that they are similar to the RS and IB neurons described in McCormick et al, 1985. This assumption is based on the high percentage of pyramidal neurons present in the *in vivo* cortex. The assumption is further supported by the similarities in firing patterns between those seen for pyramidal neurons and the experimentally observed traces in Robinson et al (1993a) and, for instance, McCormick et al (1985) or in Chagnac-Amitai and Connors (1989).

RS Neurons:

Our model for RS neurons is based on the common integrate-and-fire model for cortical RS neurons (see Liu and Wang (2001) for discussion and references). The membrane potential $v = v(t)$ in a single neuron satisfies

$$C\frac{dv}{dt} = I_{Spike} + I_{K(Ca)} + I_{Rest} + I_{Syn} + I_{Noise} \qquad (1)$$

2

where,

$$I_{Spike}(t) = -C(v_T - v_{Reset})\sum_j \delta(t - t_j) - g_R\left(1 + \frac{t - t_j}{\tau_R}\right)^{-1} P_{\gamma_j}(t - t_j)(v(t) - v_{Reset}),$$

$$I_{K(Ca)} = -g_{K(Ca)}c(v - v_K),$$

and

$$I_{Rest} = -g_L(v - v_{Reset}).$$

Here

$$P_\gamma(s) = \begin{cases} 1 & \text{for } 0 < s < \gamma \\ 0 & \text{otherwise.} \end{cases}$$

We postpone a description of the network currents, I_{Syn} and I_{Noise} for a later section. The function $c = c(t)$ is the concentration of intracellular calcium and satisfies

$$\frac{dc}{dt}(t) = c_{Step}\sum_j \delta(t - t_j) - \frac{c(t)}{\tau_c}. \tag{2}$$

The current I_{Spike} provides the integrate-and-fire spiking mechanism. Each spike time t_j is defined by $v(t_j) = v_T$ and $v'(t_j) > 0$. A spike is "pasted" on the profile of v and then v is reset to value v_{Reset}. The second term, which is refractory, is introduced to provide a prolonged refractory period to simulate the long interspike intervals which are common in RS neurons in these cultured cortical networks ($\gamma_j = t_{j+1} - t_j$). This type of device is not typical but specialized spiking has been done before in integrate-and-fire schemes (see Chow and Kopell (2001) for such a mechanism that is used to study gap junctions).

The current I_{Rest} is the usual leak current.

The current $I_{K(Ca)}$ models the K^+-current that arises from the increase in cytoplasmic calcium c during a burst event. In the defining equation for c, c_{Step} represents the influx of calcium that occurs during an AP from VGCC's (see Wang (1998) for discussion of the calcium influx).

Overall we have tried to use parameter values that are sensible with respect to those in known cortical models (see Chagnac-Amitai and Connors (1989), Liu and Wang (2001) or McCormick et al (1985)) while at the same time attempting to match experimental observations of the cultured neurons (see Opitz et al (2002), Robinson et al (1993a), or Murphy et al (1993)). For equation (1) we take $C = 180$ pF. For the spiking current I_{Spike} we assign membrane potentials $v_T = $ -30 mV and $v_{Reset} = $ -35 mV. We set the peak of an AP at $v_P = 15$ mV. For the refractory current we have $g_R = 150$ nS and $\tau_R = 12$ ms. In the K(Ca) current we have $v_K = $ -75 mV and $g_{k(Ca)} = 10.0$ nS/μM. Following Pinsky and Rinzel (1994), we make our network heterogeneous by assigning randomized values to τ_c in the equation for the calcium dynamics. Here $\tau_c = 2700$ ms is the mean and the standard deviation is 0.1 τ_c. (The value of 2700 ms seconds for τ_c was chosen from our own experimental observations, Wang and Gruenstein (1997)). We also had $c_{Step} = 100$ nM, $g_L = 8.0$ nS, and $v_{Rest} = $ -64 mV. Our $R_{in} = 125$ MΩ and time constant is $\tau_m = 23$ ms. Both of these are in ranges found experimentally; in Chagnac-Amitai and Connors (1989) R_{in} ranges from 20-190 MΩ and McCormick et al (1985) have a time constant 20.2$\pm$14.6 ms.

IB Neurons:

To model IB neurons we introduce a low threshold current which gives rise to intrinsic bursting. Our IB neurons are modeled by equation (1) and (2) with the addition of a new low threshold intrinsic current I_{LT}.

$$I_{LT}(t) = -g_{LT}(v_{Reset} - v_{Ca})\sum_j \alpha(t - t_j^{LT}; r_{LT}, \tau_{LT}). \tag{3}$$

We have used the following standard double-exponential function (Golomb and Ermentrout, 1999)) in this definition:

$$\alpha(s; r, \tau) = \frac{e^{-s/\tau} - e^{-s/r}}{e^{-\bar{s}/\tau} - e^{-\bar{s}/r}} \quad \text{where} \quad \bar{s} = \frac{r\tau \ln(r/\tau)}{r - \tau}.$$
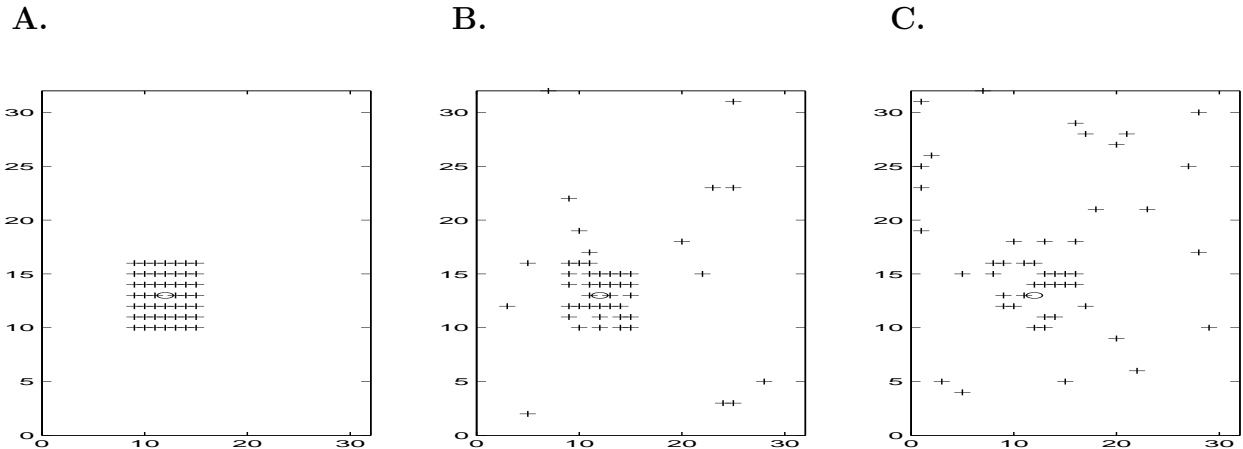
3

A. **B.** **C.**

Figure 1: Connections to a single neuron in a network of 1024 neurons. Neuron number 396 is indicated by an 'o' and the neurons it connects to (post-synaptically) are a '+'. A: Local connections with $\rho = 0.0$. B: "Small World" connections with $\rho = 0.3$. C: Highly random connections with $\rho = 0.7$.

This function rises, at first linearly, from 0 to a height of 1 in time approximately r and then decays exponentially with a time constant τ. This formula is an approximation of a Hodgkin-Huxley type current. We view this low threshold current as arising from a T-type Ca^{2+} channel which, as is typical, has an activation time constant of r_{LT} = 30 ms, an inactivation time constant of $\tau_{LT} = 180$ ms, and a depolarization threshold of $v_{LT} = $ -62 mV (Coombs et al, 2001 or Wilson, 1999). Here $v_{Ca} = 80$ mV is the reversal potential and $g_{LT} = 6.0$ nS is the conductance. While other types of low threshold currents could also be present such as a persistant sodium channel (NaP) (Mittman et al, 1997 or Traub et al, 2003), we use only the parameters characteristic of the T-type channels in the model presented here. The t_j^{LT} are, like the spike times, defined when $v(t_j^{LT}) = v_{LT}$ and $v'(t_j^{LT}) > 0$. To complete the modeling related to this low threshold current we need to account for the influx of calcium through the T-type channels. To accomplish this we add a term $f_{LT}I_{LT}(t)$ to the defining equation (2) for $c(t)$ with $f_{LT} = 1.5 \times 10^{-6}$ μM/(pA ms). This method of handling the influx of calcium is quite common; see Wang (1998).

Network Architecture:

We now define the I_{Syn} term. The synaptic current on neuron i from the network is defined in a standard way (see Humphries and Gurney (2001) for example);

$$I_{Syn}^i(t) = M_S \sum_{j \in S_i} \sum_{\ell \in F_j(t)} d_j(t)\alpha(t - t_\ell^j; r_S, \tau_S) \tag{4}$$

where the sum on j is over the neurons connected to neuron i. Here we took $M_S = 24$ pA, $r_S = 15$ ms, and $\tau_S = 300$ ms. The function $d_j(t)$ is a synaptic depression factor and is defined below. The set S_i is the set of all neuron indices that are connected to neuron i while the set $F_j(t)$ is all firing times from neuron j that occurred on or before time t. Note that the individual connection strengths, both local and global, are of equal size. The time t_ℓ^j is the time of the ℓth spike from neuron j. In figure 9 of Maeda et al (1995) most of the dendrites of the cultured neurons are around 50-100 μm long although there are some that are over 200 μm. From Opitz et al (2002) and Wang and Gruenstein (1997) we can deduce that, on average, the neurons are 25μm apart. We arranged the neurons in a $q \times q$ grid.

Following Netoff et al (2004) we have introduced a parameter $\rho \in [0, 1]$ to allow long range connections between neurons. After assembling a full local connection scheme we re-evaluate each connection; with probability ρ we break

the link and form a new connection with a randomly chosen neuron. Thus, for values of ρ close to 1 the connections become more random than local. Figure 1 has example connection schemes for small, moderate and large values of ρ. We made no special arrangements for boundary cells; thus, neurons near the center of the grid are more extensively connected than those near the edge.

Synaptic Depression:

Opitz et al (2002) argue, based on experimental data, that synaptic depression is present in these cultured networks. We introduce, for neuron j, a depression factor $d_j(t)$ which satisfies the following differential equation:

$$d_j'(t) = -\theta \sum_\ell \delta(t - t_\ell^j)d_j(t) + \frac{(1 - d_j(t))}{\tau_{SD}} \tag{5}$$

where $0 \leq \theta < 1$ and t_ℓ^j is the ℓth spike by neuron j in a burst event. This depression factor reduces the synaptic output by a fraction $1 - \theta$ with each AP but recovers over a time period on order τ_{SD}. This factor is inserted in equation (4). We note that over a time step of length Δt

$$(1 - d_j(t + \Delta t)) = (1 - \frac{\Delta t}{\tau_{SD}})(1 - d_j(t))$$

and at $t = t_\ell$, when an AP occurs,

$$d_j(t + \Delta t) = (1 - \theta)d_j(t).$$

Our motivation for this mechanism comes from reinterpreting the synaptic depression equations in, for instance, Golomb and Amitai (1997). Thus the strength of the current output from neuron j is decreased as more APs occur, loosely modeling the depletion of vesicles in a synapse. At the same time the output strength is being slowly (time constant τ_{SD} restored). We took $\theta = 0.70$ so that the mechanism turns off in a burst event in a plausible length of time. Again, we enhance the randomness of the network by taking random values for τ_{SD} with average 1.7 s and standard deviation 0.2 τ_{SD} (see for instance Tabak et al (2000)).

Noise:

We assume each neuron experiences a train of noise events which occur at randomly spaced intervals. The noise on neuron i is

$$I_{Noise}(t) = M_N \sum_k \alpha(t - t_k^N; r_N, \tau_N)$$

The t_k^N are the times determined randomly for when a noise event is to be started. We assume the α-function is not restarted until the preceeding pulse has decayed; thus $t_{\ell+1}^N > t_\ell^N + r_N + \tau_N$. We took $M_N = 35$ pA, $r_N = 30$ ms, and $\tau_N = 50$ ms. These numbers are similar to the experimentally observed major noise events in Robinson et al (1993a), (see figure 7C) and close to those assumed in Feller et al (1997). We imposed a noise event on average every $N_{Avg} = 45$ s.

Simulations:

In these simulations we approximated the solutions to the equations at times t_m with a simple Euler type method. On each step, $[t_{m-1}, t_m]$, we approximated I_{Syn}, I_{Noise}, c, and the coefficients in I_{LT} and the refractory term using their values from the previous time, t_{m-1}. We then solved the resulting linear differential equation exactly on the next time step. The package MATLAB was used in the simulations. All networks computations were on a 32×32 grid which has 1024 neurons.

3. Results:

In this section we present our computational results. In the discussion section we will place this information
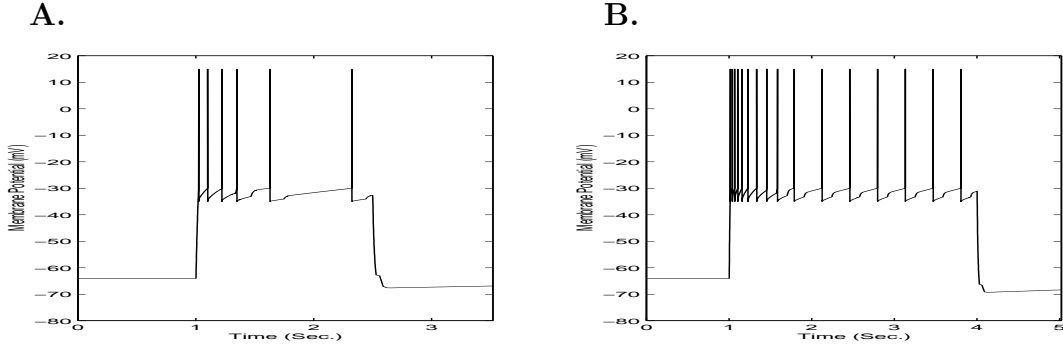
A.

B.

Figure 2: Electrical activity calculated for an isolated model RS neuron. A square pulse of current is applied at time $t = 1$ s. A: Response to a 425 pA current for 1.5 s. B: Response to a 600 pA current for 3 s.
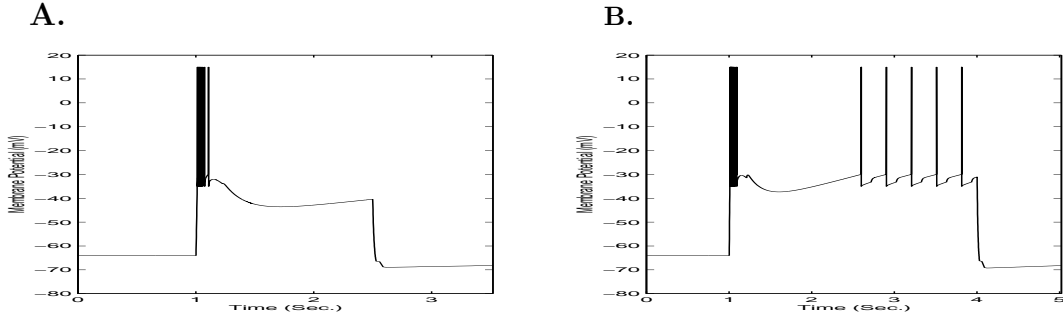

A.

B.

Figure 3: Electrical activity calculated for an isolated IB neuron. A: Response to a 425 pA current for 1.0 s started at the 1.5 s time. B: Response to a 600 pA current for 3 s started at 1 s.

into the context of the known behavior of the experimental networks and neurons.

Single Cell Dynamics:

In this subsection we study isolated RS and IB neurons. Because isolated neurons lack synapses, I_{Syn} and I_{Noise} are both zero, under these conditions no spontaneous APs will occur. However, APs and bursts of APs can occur in response to an externally applied current. Therefore, to our RS integrate-and-fire neurons we add a term I_{Appl} for an externally applied current to the membrane potential equation (1);

$$I_{Appl}(t) = M_{Appl} \ P_\tau(t - t_0)$$

with τ being the length of application, t_0 the initiation time, and M_{Appl} the amount of current. Here, P_τ is a pulse function. Figure 2A shows the response to a pulse with $\tau = 1.5$, $t_0 = 1.0$, and $M_{Appl} = 425$. Figure 2B has the response to a larger depolarizing pulse of 600 pA for 3 seconds. In the latter case the RS neuron reaches a steady rate of production of APs which stops abruptly as soon as the external current is terminated.

IB neurons behave differently due to the intrinsic current from the T-type VGCCs. Figure 3A shows the
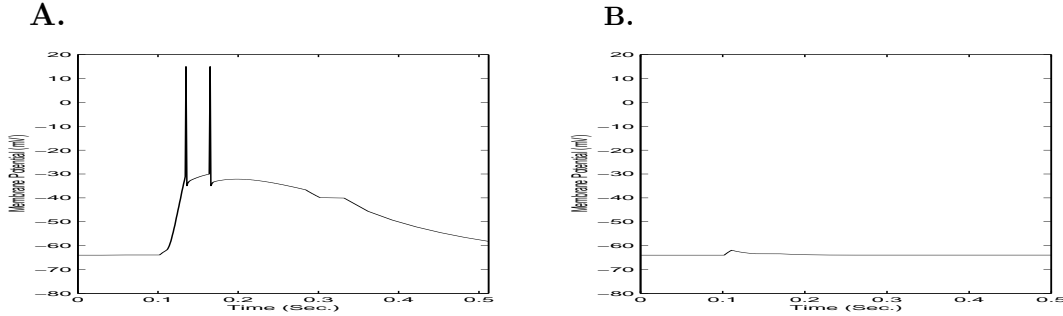
6

Figure 4: Response of IB and RS neurons to a small 50 pA current for 10 ms starting at time 0.1 s. A: Response of an IB neuron showing two AP's. B: Response of an RS neuron which has no AP's.

response of a model IB neuron to the same applied current as in figure 2A. Unlike the RS neuron, the IB neuron undergoes a short AP burst at high frequency and then produces no furthur APs. When depolarizing current is increased to 600 pA (figure 3B), the IB neurons resume firing APs at regular intervals in a similar manner to those of the RS neuron.

Of particular importance, IB neurons exhibit intrinsic bursting activity, as seen in figure 4A. When stimulated with a short 50 pA pulse of current for 10 ms, the IB cell responds with two spikes and a roughly 300 ms wide depolarization envelope. Note that the first AP occurs after the applied current pulse has ended. RS neurons did not produce any APs under these conditions nor did they exhibit a persistant depolarization (figure 4B). Furthur studies of the bursting of the IB neurons showed that the number of AP's increased as g_{LT} was increased.

The refractory mechanism in I_{Spike} changes the firing rate significantly from those seen in standard integrate-and-fire neurons. This allows our model neurons to exhibit the firing rates similar to those commonly observed in the cortex and in the cultured network experments. Note that this refractory mechanism is relative and not absolute.

We can derive a mathematical expression relating the firing rate to applied current for an RS neuron in our model network. To accomplish this, we consider the time T for the membrane potential to rise from v_{Reset} to v_T under an applied current I_{Appl} while holding the calcium concentration constant at a constant level. We can simplify equation (1) by omitting I_{Syn} and I_{Noise} and setting

$$I = I_{K(Ca)} + I_{Rest} + I_{Appl}. \tag{6}$$

Since $v - v_{Rest} \cong v_T - v_{Rest}$ and $v - v_K \cong v_T - v_K$ for v between v_{Rest} and v_T we set $v = v_T$ in the $I_{K(Ca)}$ and I_{Rest} to simplify our calculations since these currents will now be constant if c is also assumed to be constant.

It can now be shown that (see the appendix)

$$I_{Appl} = -(I_{K(Ca)} + I_{Rest}) + \frac{g_R(1 + \beta^{-1})(v_T - v_{Reset})}{(1 + T/\tau_R) - (1 + T/\tau_R)^{-\beta}} \tag{7}$$

by solving the differential equation (1) under the assumptions described above. Here $\beta = g_R \tau_R / C$ is a nondimensional constant. Taking frequency as $1/T$, we obtain from (7), with calcium concentration levels

7

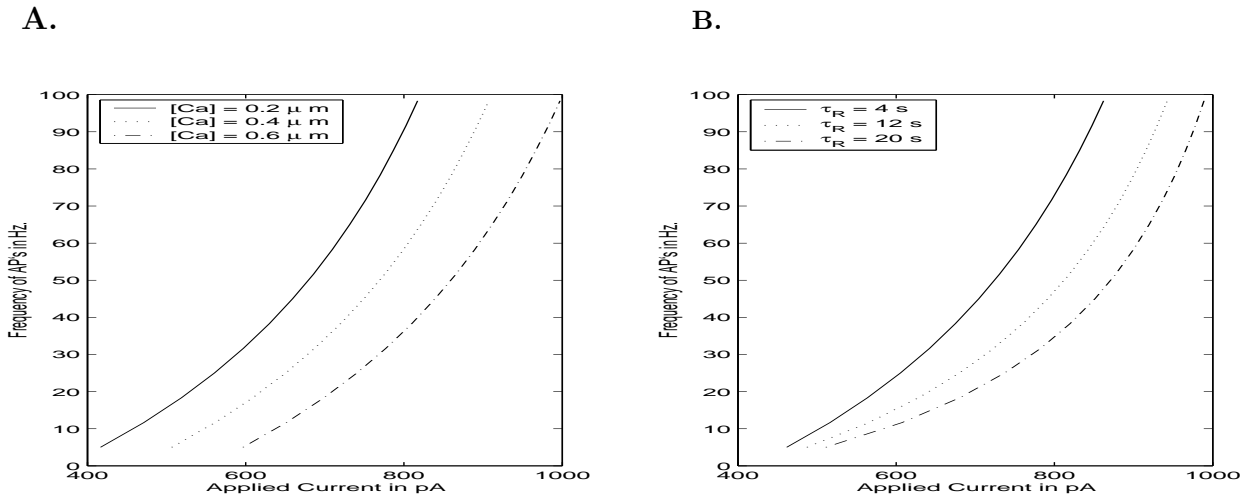**A.**   **B.**

Figure 5: Firing rate curves for integrate-and-fire model with refractory term I_{Spike}. A. Plots for different levels of cytoplasmic calcium. B. Plots for different values of refractory delay constant τ_R at $[\text{Ca}^{2+}] = 0.3\mu\text{M}$.

of $0.2, 0.4, 0.6\mu\text{M}$, the firing rate curves in figure 5A. We also explored the firing rate curves as they varied with the parameter τ_R.

The firing rates revealed in figure 5 are significantly less than those for the method without our refraction term. For example, we found that if $c = 0.3\mu\text{M}$ and $I_{Appl} = 500$ pA a standard integrate-and-fire method would have a firing rate well over 100 Hz while our new method has a rate of rougly 10 Hz (see the appendix for a figure on this). We also note that for high applied currents the firing rates tend to those for neurons without the refraction term (see appendix for an analysis of this).

Pure RS Network:

We found that networks with only RS neurons did not exhibit burst events. To bring an RS neuron to threshold the change in membrane potential would need to be nearly 30 mV. At rest the membrane potential for a single neuron, neglecting the synaptic inputs, satisfies

$$C\frac{dv}{dt} = g_L(v - v_{Rest}) + I_{Noise}.$$

If I_{Noise} were a constant then this differential equation can be solved and it can be shown that the maximum rise in v that could occur is I_{Noise}/g_L. Even if $I_{Noise} = 45$ pA, which is higher than most observed noise events, the increase in v would only be 10 mV; insufficient to initiate an AP. This explains why we were unable to identify any set of physiologically relevant parameters that would give rise to spontaneous AP bursts in our RS network.

Pure IB Network:

In contrast to RS networks, IB networks produce synchronized AP bursts and their associated calcium oscillations under a variety of conditions.

In the 20 second simulation shown in figure 6, all cells spontaneously undergo AP bursts at fairly regular
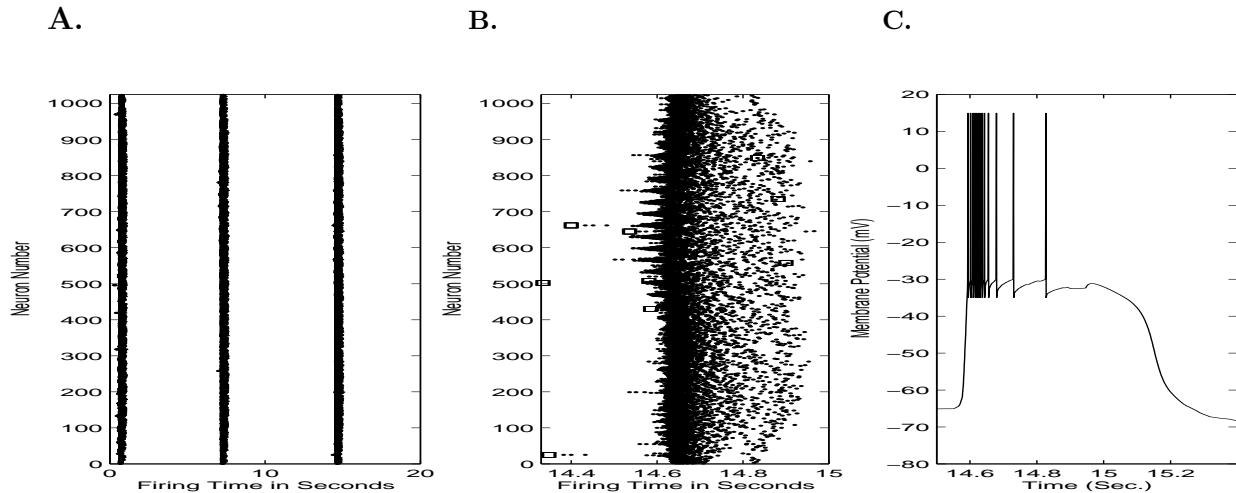
Figure 6: Synchronous behavior in a pure IB network. A: Raster plot of the burst events during the simulation. B: Raster plot of the second burst event. The boxes indicate the noise events C: Membrane potential of an IB neuron during the second burst.

intervals of approximately 6 seconds (figure 6A). Closer study of individual burst events reveals also that each burst event is initiated by a different neuron. Figure 6B displays the third burst event. Figure 6C shows the trace of the membrane potential of a typical IB neuron during a burst event. We found that the first event in figure 6A was initiated by neuron 496, the second by 258, and the third by 662 (Neuron 25 begins at nearly the same time). This pattern of random initiation events is consistent with experimental observations which have failed to find any evidence for a pacemaker (Robinson, 1993a). On the other hand, the number of AP's observed in a typical burst such as that of figure 6C is greater than what is typically observed experimentally. One obvious difference between the model and experimental system is the use of a pure IB network in figure 6. We, therefore investigated the effect of varying the fraction of IB neurons.

Networks of IB and RS Neurons:

As with pure IB networks, IB/RS networks produced synchronized AP bursts and calcium oscillations as long as the fraction of IB cells was sufficiently large. We display in figure 7 the results of an IB/RS network with 35% IB cells distributed randomly. McCormick et al (1985) have reported that 35% of neocortical pyramidal cells were of the IB type. The first, second, and third burst events are initiated by IB neuron numbers 313, 894, and 431, respectively.

Figure 7B shows a magnification of the second burst event with the IB neurons, that are spaced randomly in the simulated 2d network. They are renumbered and set in the lower spots on the raster plot so as to view them more clearly. IB neurons are seen to initiate bursting at an earlier time than RS neurons by about 0.1 seconds. Because APs have been experimentally measured in these networks only in one cell at a time we do not know whether this is occurring in cultured networks. Neither has any such dichotomy been reported in the synchrony of Ca^{2+} oscillations (Wang and Gruenstein, 1997) although it is likely that the temporal resolution of the calcium measurements was not sufficient to resolve a 100 msec difference.

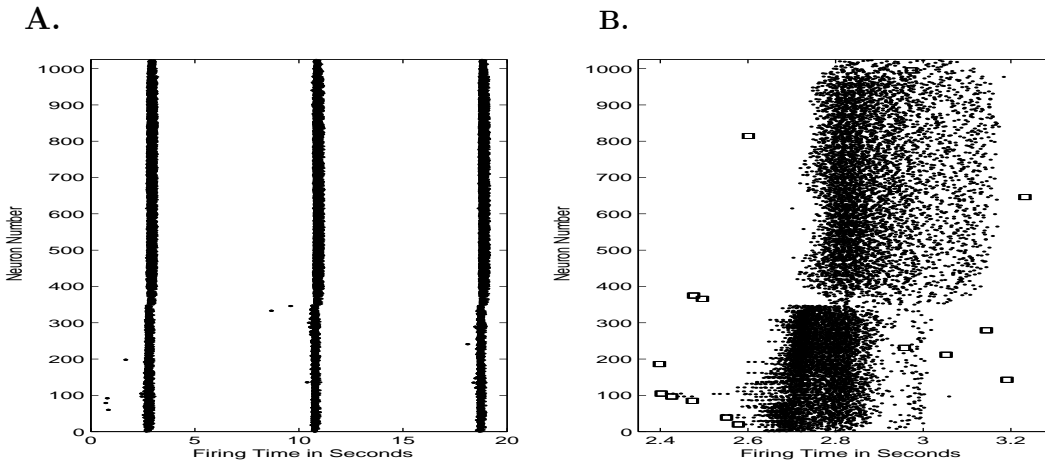Figure 8 shows the trace of the membrane potential and calcium concentration for a typical RS neuron.

Figure 7: Raster plot of the IB/RS network during an extended computation. A: All the burst events during the simulation. B: Higher time resolution view of the second burst event. The IB neurons are displayed as the first 35% of the neurons to distinguish them from the RS neurons. As before, boxes indicate noise events.

Note that the rise and fall of the calcium concentration is closely tied to the first and last AP times. The amplitude and kinetics of the calcium values are similar to what is observed experimentally in cortical neuronal cultures in which glial cells and GABAergic neurons have been depleted (our unpublished observations).

Intrinsic Bursting and Low Threshold Spiking:

We considered the effects of g_{LT}, the conductance of the IB neuron's low threshold current I_{LT} on the strength of the burst events in an IB/RS network, figure 9. We were especially interested in the case when the IB neurons only deliver one AP in response to small stimulii. Here, they could be referred to as low threshold spikers (LTSs).

We found that the IB/RS network with 35% IB doping provided full burst events even when the IB neurons were only LTSs ($g_{LT} = 4.0$ nS). So, instead, we studied networks with IB neurons placed uniformly at the nodes of the even numbered rows and columns. In this case 25% of the neurons are IB. We note this doping percentage is plausible physiologically; Chagnac-Amitai and Connors (1989) reported a mix of 17% IB and 83% RS neurons. This uniform placement of IB neurons also reduced the randomness of the network. To furthur reduce the randomness in this study we also set $\rho = 0$.

To study the effectiveness of the intrinsic bursting we stimulated a single IB neuron in the middle of the network at differing values of synaptic strength M_S and three different values for g_{LT}. Figure 9 shows the number of neurons bursting at different values of M_S for the three values of g_{LT}. As a benchmark we set M_S very low and noted the number of AP's the initiating neuron produced in response to our stimulus; this is listed in the table 1.

Table 1: AP's versus g_{LT}.

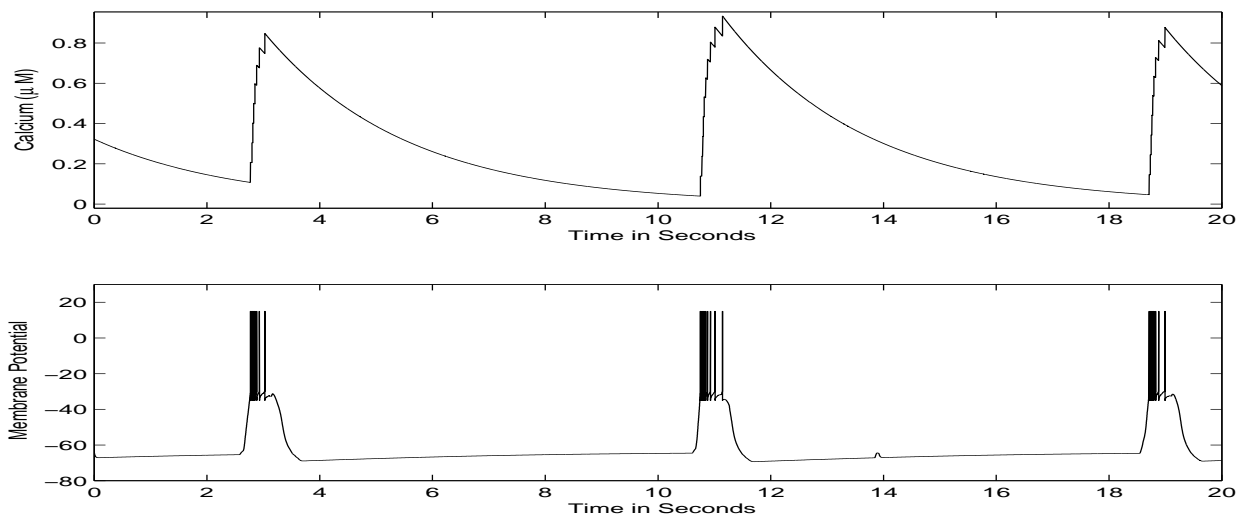| $g_{LT}(nS)$	4.0	5.2	6.2
APs	1	2	3

10

Figure 8: Correlation of AP bursts with changes in cytoplasmic calcium in an IB/RS network. On the top is the trace of the concentration of cytoplasmic calcium during the simulation. On the bottom is the trace of the membrane potential.

We also considered a pure RS network with a subset of highly active neurons. The neurons in this subset were placed, as the IB neurons were above, on the even numbered rows and columns so they accounted for 25% of the total neurons These neurons were made "active" by having their leak current set close to v_T so they could become depolarized in response to a noise event. Figure 9 shows behavior of this network under variations in M_S. For this curve a single active RS neuron is stimulated to bring on a full or partial burst event.

A somewhat unexpected result is that the IB neurons that are intrinsic with 2 APs are slightly more efficient than the 3 AP IB neurons. The AP's in the case of $g_{LT} = 6.2$ nS are delivered more quickly than those in the $g_{LT} = 5.2$ nS case. Close observation of these initiating neurons show that the initiating neuron in the $g_{LT} = 5.2$ nS case has 3 APs before the RS neurons join the burst event while the $g_{LT} = 6.2$ nS initiating neuron has 4 APs total. Because of the synaptic depression factor, $d_j(t)$ this extra AP only increases the output (presynaptic) by about 12%. Overall the $g_{LT} = 5.2$ nS IB neurons deliver nearly the same amount of current but over a longer period. This difference leads to full burst events for lower M_S values.

Wave Speed and Connection Parameter ρ:

The speed of propagation of waves of AP bursts and calcium spikes have been measured in culture and found to be in the range of 5-100 mm/s. In this section we have examined simulations of IB/RS neuron networks with 35% random doping of IB neurons. In these simulations we have suppressed the noise but do provide a short pulse to a neuron in the middle of the fourth row to initiate a burst event. By comparing the times when the neurons near the initiating neuron burst until those in the farthest rows burst, we can estimate the wave speed.

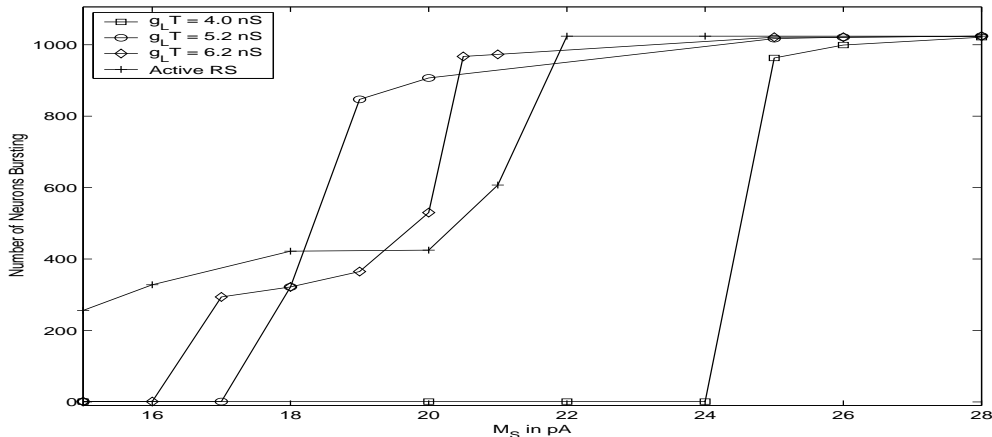In figure 10 we display the wave speed results of these simulations. We stimulated IB neuron number

11

Figure 9: Network response to variations in synaptic strength M_S and initiating neuron type. Networks with IB neuron subsets (see table 1) and an active RS neuron subset are displayed. The vertical axis measures the burst event size; the bursts were intiated by a single neuron situated in the middle of the 2-d grid.

114 which is in the lower middle of the network and then examined the burst event that then occurred. We sampled the times of the first AP for several pairs of neurons. In these pairs, one of the neurons was near the initiation site and the other far away. By assuming the rows (columns) are 25 μm apart we could compute the speed of propagation of the burst event between each of the neurons in a pair. By averaging over the pairs we obtained an estimate of wave speed. The average of speeds from five trial simulations at each value of ρ is displayed in figure 10.

As can be seen, very small increases in the small world connectivity parameter ρ profoundly effect the speed of wave propagation.

IB and RS Connection Geometry:

In this subsection we report that the geometrical configuration of the cells in mixed IB/RS networks can have a profound impact on the pattern of bursting activity. We consider a network composed of equal numbers of RS and IB neurons arranged either in alternating columns of RS and IB cells or in a checkerboard pattern. For this simulation we decreased the connectivity of the neurons so that each cell is connected only to its 8 nearest neighbors. In order to compensate for the resultant decrease in the number of synaptic inputs to each cell, we increased the strength of each synaptic connection (Here, we have $M_S = 98$ pA where M_S is the amplitude of the postsynaptic current, $\rho = 0$ and $\theta = 0.75$).

When the neurons are arrayed in a checkerboard pattern they burst with a high degree of synchrony involving up to 80% of the cells (figure 11A). Neurons arranged in alternating columns, on the other hand exhibit only small burst events which involve roughly 20% of the cells (figure 11B). The reason underlying the difference in behavior of the two geometries relates primarily to the connectedness of the IB neurons. In the checkerboard a connected path can be found between any two IB neurons in the network. In the columnar geometry, the IB cells of one column do not connect directly to any other IB cells, but rather must first pass through the cells of an adjacent RS column.

In particular, in the columnar geometry, when an IB neuron fires, only one column of IB neurons is
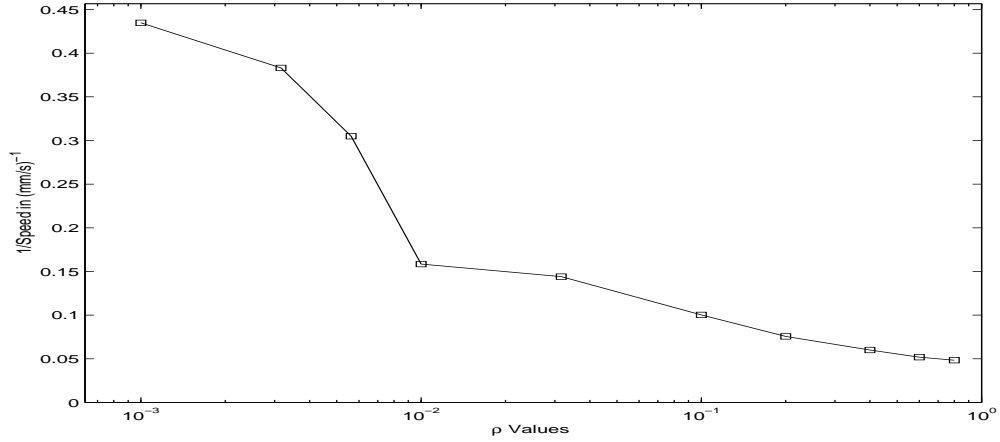
12

Figure 10: Estimated inverse wave speeds of IB/RS network with 35% random IB doping depending on the small-world parameter ρ.
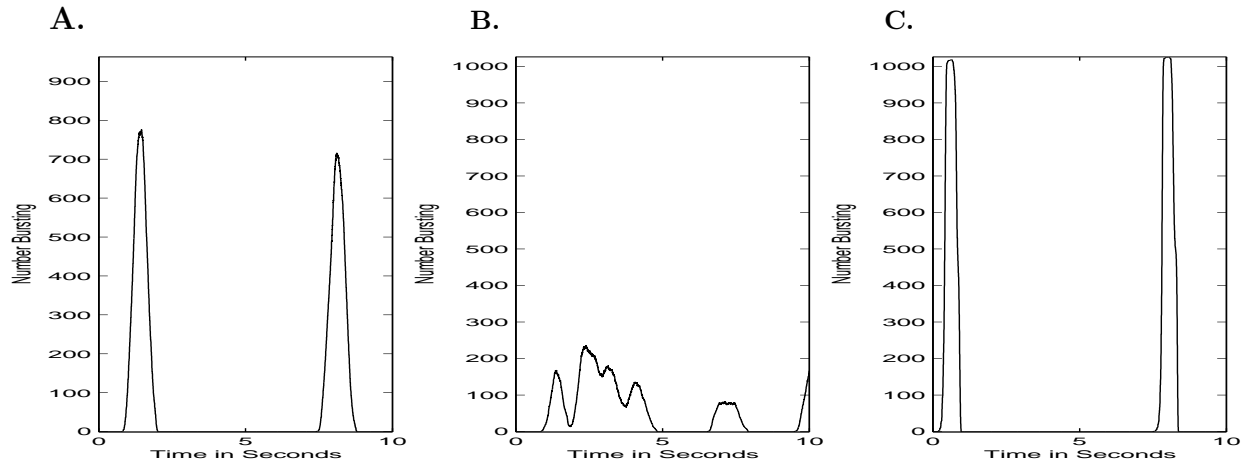

Figure 11: IB/RS network response to changes in geometry. A: Checkerboard pattern with $n = 961$. B: Columnar pattern with $n = 1024$. C: Columnar pattern with small world connections ($\rho = 0.4$).

13

activated. Other columns of IB neurons cannot respond to this activation unless some of the RS neurons in the intermediate columns begin to burst. This will only occur if the synaptic current from *three* neighboring IB neurons is sufficient to bring an RS neuron to threshold.

In contrast, in the checkerboard geometry, all IB neurons fire when at least one is activated since the groups of IB's are not isolated as they were in the columnar case. In this situation the RS neurons are more likely to be activated since they are connected to *four* firing IB neurons. Overall we found that for $M_S << 98$ pA neither network had full burst events while for $M_S >> 98$ pA both networks had full burst events.

To restore the synchronous bursting in the network with columnar geometry we let $\rho = 0.4$ (figure 11C).

Deactivation Mechanisms:

We also tried removing deactivation mechanisms. When we set $\theta = 1$, effectively eliminating synaptic depression we obtain a persistant firing state; this occurred because the AHP current was no longer sufficient to deactivate the burst event. When we set $g_{AHP} = 0$ nS effectively removing the I_{AHP} current, (and reinstating $\theta = 0.70$) we found that the burst events were greatly extended in time but the synaptic depression was able to deactivate the burst event.

4. Discussion:

We have introduced a new integrate-and-fire neuronal network model with two-dimensional geometry and a small world connection scheme. This computer model was developed primarily to mimic the spontaneous electrical bursting and synchronized calcium oscillations observed experimentally in cultured cortical neuronal networks (see references listed in the introduction). The model contains two types of neurons, RS and IB, which differ from each other in the absence or presence, respectively, of a low threshold current that mimics a persistent Ca^{2+} current. Other features that, *in aggregate*, distinguish this from previous integrate-and-fire network models are a calcium activated K^+ current $I_{K(Ca)}$, a mechanism for deactivating synaptic depression, two-dimensional geometry, a small world connection scheme, and an AP refractory current.

Without the refractory current term in I_{Spike} and the deactivation current $I_{K(Ca)}$ the many similarities observed between single neuron data generated by the computer model and experimental data would not have been obtained. Such similarities were observed for a variety of situations. For example, the generation of burst activity by a 425 pA step current observed in cortical neurons (see fig 5C in Robinson, et al (1993a)) closely mimics the response of an isolated RS neuron seen in figure 2A. Burst patterns closely resembling those of the IB neuron in figure 3 have been observed by Chagnac-Amitai and Connors (1989), McCormick, et al (1985) and Schwindt and Crill (1999). Firing rates of 10-20 Hz are commonly observed in cultured networks of cortical neurons (see Robinson, et al (1993) or Opitz, et al, (2002)), whereas in the in vivo neocortex firing rates of 70-100 Hz have been observed (McCormick, et al (1985). The magnitude of the firing rates seen in figure 5 compare favorably to these values under a physiological range of calcium concentrations and applied currents.

In terms of network behavior, features such as the synchronization of calcium oscillations, the close association of the rising phase of each calcium spike with the AP bursts and the absence of any evidence for a pacemaker, the data of figures 6-8 are in agreement with experimental observations (see Robinson, et al (1993) and Opitz, et al (2002). The random nature of the initiation sites that are observed experimentally and in our model is similar to that in Butts and Feller (1999).

The refractory term in I_{Spike} was chosen so as to retain the depolarization envelope commonly observed in bursting neurons. We note that other decay functions such as an exponential could have been used for the refractory term instead of the $(1 + (t - t_j)/\tau_R)^{-1}$ that we chose. However, as shown in the appendix this

rational function leads, in a straightforward way, to a closed form formula for the firing rate.

Our study demonstrates that the intrinsic bursting tends to enhance the capability of the network to initiate full burst events (see results in figure 9). In order to determine whether IB neurons were required we also studied pure RS networks with a subset of neurons having a high resting potential. However, the behavior of this network differed from that of a mixed IB/RS network as is also seen in figure 9. Our conclusion is that while using low threshold cells can give rise to spontaneous synchronized bursting, the network behavior is not identical to the situation where fully intrinsic IB neurons are used. As noted earlier, there is considerable experimental evidence for the presence of such in vivo IB neurons (see Chagnac-Amitai and Connors (1989) or McCormick et al (1985)).

There is increasing evidence that small world schemes are more representative of physiological conditions (see Shefi, et al (2002) or Strogatz (2001)). When small world connection schemes are used in our model, even when connectivity is increased only slightly above $\rho = 0$, values for the speed of propagation can be obtained that fall well within the range of physiological values (5-100 mm/s) observed by Maeda, et al (1995). A similar increase in wave speed with the addition of long range connections was observed in Compte, et al (2003). A more general approach to the phenomenon of the speed of communication as a function of small world connectivity has been studied by Watts and Strogatz (1998) and our figure 10 bears a close resemblance to their figure 3B.

Interestingly, however, reduction of the small world scheme to its most basic level in which each neuron is connected only to its 8 nearest neighbors (i.e. $\rho = 0$), can lead to a dichotomy of responses that depends on the geometry of the RS and IB cells, as shown in figure 11. These results are in agreement with ideas proposed by Strogatz that the imposition of even a small amount of random connectivity is capable of restoring global communications. It is possible that similar geometric constraints could be employed in vivo to restrict or promulgate communications among populations of neurons.

We note that when the work in this paper is viewed as a generic model of neuronal network behaviour our simulations are quite similar to those in Compte et al (2003), Feller et al (1997), Golomb (1998), and Wiedemann and Lüthi (2003). However, our model differs from Compte et al (2003) and Golomb (1998) since it is an integrate-and-fire model and is placed in a two-dimensional arrangement. It differs from Wiedemann and Lüthi (2003) because of the two-dimensional geometry and also because of the incorporation of noise events, more specialized firing patterns, and the intrinsic bursting property of our IB neurons. Our integrate-and-fire neurons are more complex than those in Feller et al (1997).

We neglected inhibitory neurons in our study. Our own (unpublished) experimental work and the research of Opitz et al (2002) and Robinson et al (1993) indicate inhibitory synapses are present and do play a role in the synchronous activity. In particular, Voigt, et al (2001), have proposed that oscillations in cortical networks are driven by GABAergic neurons. This raises the question of how such oscillations can be generated in our model. However, in a separate study, we have found that in cultures that have been treated with cytosine arabinoside to kill small GABAergic neurons and in which all remaining GABAergic receptors are inhibited pharmacologically, calcium oscillations still occur, albeit at reduced frequency (our unpublished data).

References:

Butts and Feller (1999), J. Comp. Neurosci. 19: 3580-

Chow CC and Kopell N (2000), Dynamics of spiking neurons with electrical coupling, *Neural Computation* 12: 1643-78.

Chagnac-Amitai Y and Connors BW (1989), Synchronized excitation and inhibition driven by intrinsically bursting neurons in the neocortex, *J. Neurophysiol.* 62: 1149-1162.

Compte A, Sanchez-Vives MV, McCormick DA, Wang X-J (2003), Cellular and network mechanisms of slow oscillatory activitiy (< 1 Hz) and wave propagations in a cortical network model, *J. Neurophysiol* 89: 2707-2725.

Connors BW, Gutnick MJ, Prince DA (1982), Electrophysical properties of neocortical neurons in vitro, *J. Neurophysiol.* 48: 1302-1320.

Coombs S, Owen MR, Smith GD (2001), Mode locking in a periodically forced integrate-and-fire-or-burst neuron model, *Physical Review E* 64: 041914.

Fall CP, Marland ES, Wagner JM, Tyson JL, *Computational Cell Biology*, Springer-Verlag (2002).

Feller MB (1999), Spontaneous correlated activity in developing neural circuits, *Neuron* 22: 653-656.

Feller MB, Butts DA, Aaron HL, Rokhsar DS, Shatz CJ (1997), Dynamic processes shape spatiotemporal properties of retinal waves, *Neuron* 19: 293-306.

Golomb D (1998), Models of neuronal transient synchrony during propagation of activity through neocortical circuitry, *J. Neurophysiol.* 79: 1-12.

Golomb D and Amitai Y (1997), Propagating neuronal discharges in neocortical slices: computational study, *J. Neurophys.* 78: 1199-1211.

Golomb D and Ermentrout GB (1999), Continuous and lurching traveling pulses in neuronal networks with delay and spatially decaying connectivity, *PNAS* 96: 13480-13485.

Humphries MD and Gurney KN (2001), A pulsed neural network model of bursting in the basal ganglia, *Neural Networks* 14: 845-863.

Katz LC and Schatz CJ (1996), Synaptic activity and the construction of cortical circuits, *Science* 274: 1133-1138.

Laing CR and Longtin A (2002), A two variable model of somatic-dendritic interations in a bursting neuron, *Bulletin of Mathematical Biology* 64: 829-860.

Liu Y-H and Wang X-J (2001), Spike-frequency adaptation of a generalized leaky integrate-and-fire model neuron, *J. Comput. Neurosci.* 10: 25-45.

Maeda E, Robinson HPC, A. Kawana K (1995), The mechanisms of generation and propagation of synchronized bursting in developing networks of cortical neurons, *J. Neuroscience* 15: 6834-6845.

Mittmann T, Linton SM, Schwindt P, Crill W (1997), Evidence for persistant Na^+ current in apical dendrites of rat neocortical neurons form imaging of Na^+-sensitive dye, *J. Neurophysiol.* 78: 1188-1192.

Murphy TH, Blatter LA, Wier WG, Baraban JM (1992), Spontaneous synchronous synaptic calcium transients in cultured cortical neurons, *J. Neurosci* 12: 4834-4845.

McCormick DA, Connors BW, Lighthall JW, D.A. Prince DA (1985), Comparative electrophysiology of pyramidal and sparsely spiny stellate neurons of the neocortex, *J. Neurophysiol.* 54: 782-806.

Netoff TI, Clewley R, Arno S, Keck T, and White JA (2004), Epilepsy in small-world networks, *J. Neurosci* 24: 8075-8083.

Opitz T, de Lima AD, Voigt T (2002), Spontaneous development of synchronous oscillatory activity during maturation of cortical networks in vitro, *J. Neurophysiol.* 88: 2196-2206.

Pinsky PF and J. Rinzel J (1994), Intrinsic and network rhythmogenesis in a reduced Traub model, *J. Comput. Neurosci.* 1: 39-60.

Robinson HPC, Kawahara, Jimbo MY, Torimitsu K, Kuroda Y, Kawana A (1993a), Periodic synchronized bursting and intracellular calcium transients elicited by low magnesium in cultured cortical neurons, *J. Neurophysiol.* 70: 1606-1616.

Robinson HPC, Torimitsu K, Jimbo Y, Kuroda Y, Kawana A (1993b), Periodic bursting of cultured neurons in low magnesium: cellular and network mechanisms, *Jap. J. Physiol.* 43 (Suppl. 1): S125-S130.

Schwindt P and Crill W (1999), Mechanisms underlying burst and regular spiking evoked by dendritic depolarization in layer 5 cortical pyramidal neurons, *J. Neurophysiol.* 81: 1341-1354.

Shefi O, Golding E, Segev, R, Eshel B-J, and Ayali A (2002), Morphological characterization of *in vitro* neuronal networks, *Phys. Rev. E* 66: 021905(5)

Strogatz SH (2001), Exploring complex networks, *Nature*, 410: 268-276.

Tabak J, Senn W, O'Donovan MJ, Rinzel J (2000), Modeling of spontaneous activity in developing spinal cord using activity-dependent depression in an excitatory network, *J. Neurosci.*, **20** , 3041-3056.

Traub RD, Buhl EH, Gloveli T, Whittington MA (2003), Fast rhythmic bursting can be induced in layer 2/3 cortical neurons by enhancing persistent Na^+ conductance or by blocking BK channels, *J. Neurophysiol.* 89: 909-921.

van Vreeswijk C and Hansel D (2001), Patterns of synchrony in neural networks with spike adaptation, *Neural Computation* 13: 959-992.

Voigt T, Opitz T, de Lima AD (2001), Synchronous oscillatory activity in immature cortical network is driven by GABAergic preplate neurons, *J. Neurosci.* 21: 8895-8905.

Wang X-J (1998), Calcium coding and adaptive temporal computation in cortical pyramidal neurons, *J. Neurophysiol.* 79: 1549-1566.

Wang X-S and Gruenstein E (1997), Mechanism of Synchronized Calcium Oscillations in Cortical Neurons, *Brain Res.* 767: 239-249.

Watts DJ and Stogatz SH (1998), Collective dynamics of 'small world' networks, *Nature* 393: 440-442.

Wilson HR (1999), Simplified dynamics of human and mammalian neocortical neurons, *J. Theor. Biol.* 200: 375-388.

Wiedemann UA and Lüthi A (2003), Timing of synchronization by refractory mechanisms, *J. Neurophysiol.* 90: 3902-3911.

Appendix:

In this section we estimate the firing rate of our scheme for constant calcium concentration c; that is, we find the first time T so $v(T) = v_T$ where

$$C\frac{dv}{dt} = \frac{g_R}{1 + t/\tau_R}(v - v_{Reset}) + I \ \text{ and } \ v(0) = v_{Reset}$$

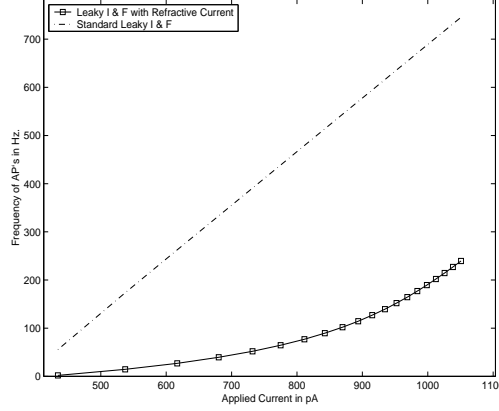Figure 12: Firing rate curves for leaky integrate-and-fire methods with and without the refractory term in I_{Spike} at $[\text{Ca}^{2+}] = 0.3\mu\text{M}$

and I is defined by (6); this will provide the formula (7). Here I_{Appl} is the applied current, we have taken $v = v_T$ in the second two currents, and c is constant in $I_{K(Ca)}$ (again, see (6). Setting $w(t) = v(t) - v_{Reset}$, dividing by C, and using β, as defined in the firing rate section, the initial value problem (IVP) becomes

$$w' + \frac{\beta}{\tau_R + t}w = \frac{I}{C}, \text{ and } w(0) = 0.$$

This is a standard linear IVP which can be solved; setting $w(T) = v_T - v_{Reset}$ we obtain

$$v_T - v_{Reset} = \frac{\tau_R I}{C(\beta + 1)}\left[(1 + T/\tau_R) - (1 + T/\tau_R)^{-\beta}\right]$$

Rearranging and solving for I_{Appl} gives equation (7).

We, furthur, note that for high firing rates when $T/\tau_R << 1$,

$$(1 + \frac{T}{\tau_R})^{-\beta} \cong 1 - \beta\frac{T}{\tau_R}.$$

Then (7) can be simplified to

$$I_{Appl} = -(I_{Rest} + I_{K(Ca)}) + \frac{C(v_T - v_{Reset})}{T}.$$

As $T \to 0$ it now follows that

$$I_{Appl} \to \frac{C(v_T - v_{Reset})}{T}$$

which is the same limit as would be obtained for the firing rate of equation (1) when these is no refraction term and c is held constant.

Finally, we note that figure 12 displays firing rate curves for the integrate-and-fire method with and without the refraction term.